Mechanism of Cis-to-Trans Isomerization of Azobenzene: Direct MD Study

Tsutomu Ikegami,*,† Noriyuki Kurita,†,‡ Hideo Sekino,‡ and Yasuyuki Ishikawa†

Department of Chemistry, University of Puerto Rico, P.O. Box 23346, UPR Station, San Juan, Puerto Rico 00931-3346, and Department of Knowledge-Based Information Engineering, Toyohashi University of Technology, Toyohashi, Aichi 441-8580, Japan

Received: December 12, 2002; In Final Form: April 2, 2003

The thermal isomerization reaction of *cis*-azobenzene to its trans isomer has been studied by direct molecular dynamics. The semiempirical PM3 method was used to calculate the force field, which was verified by density functional (PW91) calculations. The transition state for the reaction was searched by both methods. The trajectories were started from the transition state dressed with zero-point vibration, and the transient vibrational spectrum was collected. Two types of the vibrational modes were found to be excited at 1 ps, both of which correspond to in-plane skeletal vibration of the benzene ring (ν_8 and ν_{19}). The lifetimes of those modes are estimated to be 1.2 and 1.8 ps, respectively. The results indicate that ν_8 and ν_{19} modes of the benzene ring play an important role in the thermal isomerization.

I. Introduction

Azobenzene is the prototype of a group of aromatic molecules in which two benzene rings are connected by an azo group. There are trans and cis isomers with respect to the azo group. The trans isomer is more stable and isomerizes to cis isomer on irradiation. Thus-formed cis isomer slowly undergoes thermal reversion to the trans conformation. This photochromic cycle of azobenzene and its derivatives has drawn considerable attention, both applied and fundamental, for decades.[1] Among the notable studies, Jiang and Aida reported that the cis-to-trans isomerization rate of a high-order azodendrimer was greatly enhanced by infrared irradiation.[2] The azodendrimer is a treelike polymer in which the azobenzene core sits in the center surrounded by a highly branched polymer shell. They found that mild excitation on a specific infrared band, namely, a stretching vibrational band for aromatic rings (1597 cm^{-1}), accelerates the isomerization by a factor of several hundreds. Their observation strongly suggested that intermittent photon absorption accumulates to overcome the potential energy barrier of the isomerization. Judging from the irradiation condition, however, the vibrational relaxation rate is well faster than the interval of photon absorption, and the accumulation of the photon energy seems to be improbable. In an effort to shed light on the subject, we have chosen to begin with the detailed mechanism of the thermal isomerization reaction of *cis*-azobenzene.

There are two possible mechanisms for the isomerization reaction. One is the inversion mechanism, in which one N═N−C bond angle increases to form the isomer, keeping the C−N═N−C atoms planar. The other is the rotation mechanism, in which the C−N═N−C dihedral angle changes to isomerize, as is common in the photochemistry of olefins. Both experimentally[3,4] and theoretically,[5−8] it is evident that the thermal cis−trans isomerization of azobenzene proceeds via the inversion mechanism. Andersson et al. measured the cis-to-trans isomerization rate in the gas phase[3] and determined the activation energy to be 1.22 eV. They compared the value with the CNDO-calculated activation energy[5] and confirmed the inversion mechanism. A CIPSI calculation with 3-21G basis set was done by Cimiraglia and Hofmann.[6] They also found that the inversion mechanism is favored and found an activation energy of 1.05 eV. Much more elaborate calculations have recently been done. Cattaneo and Persico[7] used multireference perturbation theory with a basis set of moderate size. They drew potential energy curves of the ground and several excited states along a prefabricated reaction path and found that the potential energy barrier was smaller for the inversion mechanism (1.45 eV). Ishikawa et al.[8] mapped the potential energy surfaces of several low-lying electronic states with the CASSCF method, again showing the preference for the inversion mechanism. All of the studies mentioned above, however, were concerned with azobenzene in equilibrium, and there is little information on the dynamics of the reaction. Very recently, several experiments[9,10] have been conducted to resolve the short-time behavior of the isomerization reaction, but they focused on the effect of reaction on the electronic excited states.

In the present study, we have investigated the dynamical aspect of the isomerization reaction on the electronic ground state using the direct molecular dynamics (MD) method.[11] In direct MD calculations, no a priori fitting of the potential energy surface to a simpler functional form is performed. Instead, the potential energy and its gradient are evaluated point-by-point during the course of each trajectory. In the next section, the details of the MD calculation is described along with the method used to calculate the vibrational spectra from the trajectories. The results are shown in section III, followed by discussions. Section V is devoted to conclusions.

II. Calculation

A. Molecular Dynamics. The semiempirical molecular orbital method (PM3 model)[12] was employed to calculate the potential energy and its gradient for the direct MD calculations on azobenzene. A limited number of trajectories were also

* To whom correspondence should be addressed. Present address: Grid Technology Research Center, AIST Tsukuba Central 2, Tsukuba 305-8568, Japan.

† University of Puerto Rico.

‡ Toyohashi University of Technology.

10.1021/jp027707n CCC: $25.00
Published on Web 05/13/2003

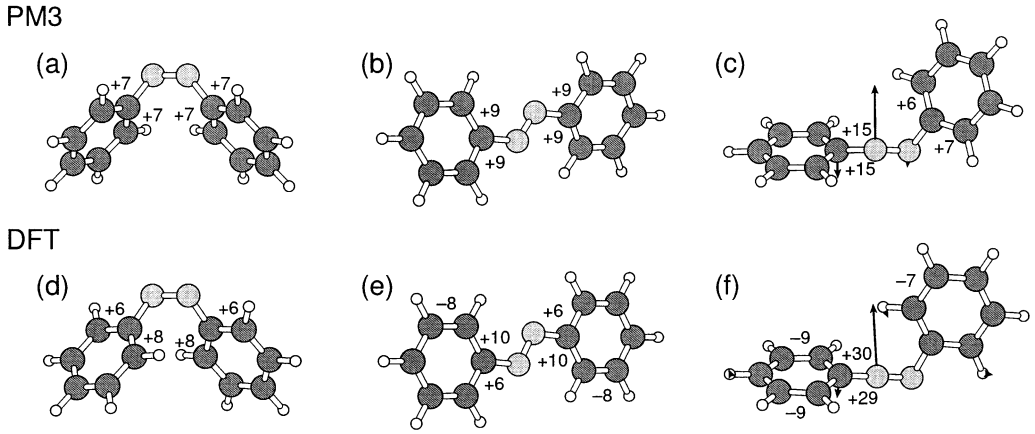

Figure 1. The stationary structures of azobenzene: (a, d) *cis*-azobenzene; (b, e) *trans*-azobenzene; (c, f) the transition state connecting them. Structures a−c were optimized at the PM3 level, while structures d−f were done at the DFT (PW91/6-31G(d)) level. The deviations of the C−C bond length from those in benzene (1.391 and 1.402 Å for PM3 and DFT, respectively) are indicated in millangstrom units, if they are larger than 5 mÅ. The arrows in structures c and f indicate the normal mode with imaginary frequency, which is the reaction coordinate for the isomerization reaction.

calculated with the density functional theory (DFT), where PW91 exchange/correlation functionals[13] and 6-31G(d) basis sets were used. The vibrational frequencies and the indices of the normal modes, ascending order starting from 1, discussed below were calculated at PM3 level, unless otherwise noted.

The numerical integration of the equations of motion was performed by using the fourth-order symplectic integrator by Martyna and Tuckerman (M−T).[14] In the present MD calculations, an integration step of 0.76 fs was employed, instead of the typical value of 0.5 fs used with Verlet method. The preparation of extended phase-space coordinates, such as $J = \mathrm{d}F/\mathrm{d}t$, $K = \mathrm{d}J/\mathrm{d}t$, and $L = \mathrm{d}K/\mathrm{d}t$, where F is the force, are required in the M−T algorithm. Those auxiliary variables were obtained numerically from five-point polynomial interpolation. Two forward and two backward trajectory points were generated using the velocity Verlet method with one tenth of the integration step width. Note that the calculation cost for one integration step in the M−T algorithm is the same as it is in Verlet method, except for the preparation at the startup and extra storage for the auxiliary variables during the calculation.

The initial conditions were selected such that the trajectory starts from the transition-state structure of the cis-to-trans isomerization reaction. After preliminary tests, it was found that isomerization typically requires trajectories that are too long to be practical if started from a cis stable structure. Either an artificial setup of the initial conditions or very high temperature was needed to force reaction. For this reason, we limited ourselves to the half-reaction from the transition structure to the cis conformation. The velocity to simulate zero-point vibrational motion was added to each bound mode at the transition state. The direction of the velocity was taken randomly. There are 65 bound vibrational modes at the transition state, so the possible directions of the initial velocity are 2^{65}. The sum of the zero-point energies at the transition state was 5.10 and 5.01 eV for PM3 and DFT calculations, respectively. Another velocity of 50 meV was imparted along the reaction coordinate for the half-reaction to proceed toward the cis conformation.

The Gaussian 98 package[15] was used to calculate energy, force, and vibrational frequencies, as well as to locate the transition state. The semiempirical MO program MOPAC2000[16] was also used in part to calculate the PM3 forces.

B. Transient Vibrational Spectrum. The transient vibrational spectrum after isomerization to the cis conformation was calculated from the velocity autocorrelation function. The origin of time, $t = 0$, was taken to be the time of passage through the transition state, that is, at the start of the trajectory calculation. The transient spectrum at time t was calculated from the segment $t \pm 0.39$ ps (1024 steps) of the trajectory.

The vibrational spectrum was calculated from the Fourier transformation of the mass-weighted velocity autocorrelation function,

$$E(\nu) = \sum_k \frac{m_k}{t_\mathrm{f} - t_\mathrm{i}} \left| \int_{t_\mathrm{i}}^{t_\mathrm{f}} v_k(t)\, \mathrm{e}^{-2\pi i \nu t}\, \mathrm{d}t \right|^2 \qquad (1)$$

where $E(\nu)$ is the kinetic energy density as a function of the frequency, t_i and t_f mark the period used for the analysis, v_k and m_k are the Cartesian velocity and the mass, and the subscript k runs over the 72-dimensional coordinate. Thus-obtained $E(\nu)$ is a transient vibrational spectrum at time t after the trans-to-cis isomerization reaction takes place, or in reverse, at time t before the cis-to-trans isomerization reaction.

The calculation of the transient spectrum is intended to search for the conditions under which isomerization takes place. Needless to say, large amplitude motion is required. Preliminary MD calculations starting from the cis conformation, however, demonstrated that large amplitude motion alone is not sufficient. Even though the molecule is deformed to near the transition state, it readily slips into other cis structures. The present analysis will find out which assisting modes, if they exist, must be excited to induce the system to cross the transition barrier.

III. Results

A. Stationary Points. The stationary structures of azobenzene were located by both PM3 and DFT. The stable structures for cis and trans isomers, as well as the transition state connecting them, were located. All stationary points were verified by frequency analysis. The structures are depicted in Figure 1, and their energies and structural parameters are summarized in Table 1. We have also calculated DFT stable structures with diffuse function added to the basis sets (PW91/6-31+G*), but no notable changes were observed.

Comparing the PM3 results with DFT, the PM3 method works fairly well considering its minimal calculation cost. The stability of the trans isomer is underestimated by PM3, which would be a problem if we were studying isomerization from

TABLE 1: Relative Energies and Structural Parameters for *cis*- and *trans*-Azobenzenes and the Transition State between Them[a]

method	energy (eV)	N=N (Å)	C−N (Å)	N=N−C (deg)	C−N=N−C (deg)	N=N−C−C (deg)
			cis-Azobenzene			
PM3	0.000	1.216	1.451	128.2	0.0	67.4
DFT	0.000	1.261	1.433	123.9	12.0	47.5
			trans-Azobenzene			
PM3	−0.093	1.231	1.447	119.8	180.0	13.2
DFT	−0.588	1.276	1.417	114.2	180.9	0.0
			Transition State			
PM3	1.179	1.210	1.380[b]	176.6[b]	90.2[d]	*e*
			1.467[c]	120.9[c]		43.7
DFT	1.010	1.238	1.331[b]	178.9[b]	72.9[d]	*e*
			1.454[c]	116.5[c]		1.0

[a] The structures obtained by PM3 and the density functional theory (DFT; PW91/6-31G(d)) are compared. [b] Flipping side. [c] Spectator side. [d] Dihedral angle of C−C(flipping)−(N=)N−C(spectator). [e] Indefinable.

the trans side, but the barrier height from the cis side is acceptable. There is a marked difference in the rotation angle of benzene rings (N=N−C−C dihedral angles listed in the last column in Table 1). However, these angles are associated with low-frequency vibrational modes, all below 110 cm^{-1}, and an exact value would require a much higher level of calculation. Indeed, the nonplanar structure of *trans*-azobenzene was obtained at the MP2/6-31+G* level,[17,18] and it agrees well, perhaps fortuitously, with the PM3 result. Differences in the low-frequency modes are likely to be irrelevant in the MD calculations because the exothermicity of the half-reaction is more than 1 eV ($\simeq$ 8000 cm^{-1}).

B. Verification of Integrator. The accuracy and efficiency of Martyna and Tuckerman's integrator (the M−T method) was verified against the velocity Verlet method by the present MD simulations. The test trajectory starts from the cis stable structure, and velocities were set up to force the isomerization reaction. That is, about 2 eV of kinetic energy was deposited into each of the second and fifth vibrational modes, besides the velocities simulating the zero-point vibration. Because the zero-point energies of *cis*-azobenzene/PM3 sum to 5.15 eV, the total kinetic energy of the molecule amounted to 9.17 eV. Isomerization occurred at $t = 0.4$ ps.

Trajectories were calculated by both methods with three different integration steps, 0.51, 0.76, and 1.02 fs. The total energy is plotted as a function of time in Figure 2a. The M−T method gives a satisfactory result if the integration step is less than 0.76 fs. Indeed, the total energy is conserved better for M−T/0.76 fs than for Verlet/0.51 fs. If the integration step is increased to 1.02 fs, however, the energy fluctuation in the M−T method becomes worse. Nevertheless, the total energy fluctuates in a limited regime and does not increase or decrease with time because of the symplectic property of the integrator.

The accuracy of the integrator is examined in Figure 2b, in which the discrepancy of the calculated trajectory from the reference is plotted as a function of time. The discrepancy is defined as distance from the reference structure in the 72-dimensional conformational space. A Verlet trajectory with integration step of 0.10 fs was used as a reference trajectory. Much better results were obtained for the M−T algorithm if M−T/0.10 fs trajectory was used as a reference; Verlet/0.10 fs was chosen to provide severe test. It is obvious from the figure that the M−T method is much more accurate than the Verlet method. Even the M−T/1.02 fs trajectory is more accurate than Verlet/0.51 fs, despite the large energy fluctuation. In the present

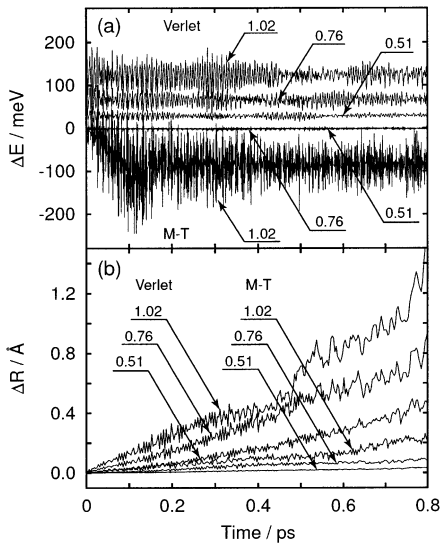

Figure 2. Comparison of numerical integrators, velocity Verlet method and Martyna−Tuckerman method. The numbers within the figures indicate the integration step in femtoseconds. In panel a, the total energy (potential + kinetic) is plotted as a function of time. In panel b, The discrepancy from the reference trajectory is plotted as a function of time. The distance in the 72-dimensional conformation space is used in the plot. The reference trajectory was calculated by the velocity Verlet method with an integration step of 0.1 fs.

application, however, the integration step of 0.76 fs was chosen to enhance the energy conservation.

C. Transient Vibrational Spectrum. One hundred trajectories were calculated, starting from the transition state for as long as 10.7 ps, and the transient vibrational spectra were derived from them. The deviation of the total energy of the trajectories is between 30 and 70 meV. The transient spectra, $E(\nu)$, were calculated at $t = 1$ ps for each trajectory. The segment from $t = 0.61-1.39$ ps was used, which roughly corresponds to the second cycle of the large amplitude vibration, namely, flapping of the benzene rings. The spectra were averaged over 100 trajectories and are shown in Figure 3a. The resolution of the spectrum is as low as 40 cm^{-1} because of the short period of 0.78 ps used to calculate $E(\nu)$. The ergodic spectrum, in which the available energy is distributed equally among all of the normal modes of *cis*-azobenzene, is also plotted. To simulate the spectrum, Gaussian line shapes of 40 cm^{-1} width were placed at each vibrational frequency of *cis*-azobenzene. The available energy of 6.32 eV was divided into 66 normal modes, and half was assumed to go into the kinetic energy. The ergodic spectrum thus obtained is proportional to the vibrational-state density distribution at the cis stable structure. The averaged spectrum is almost identical to the ergodic one, except that it is slightly shifted to lower wavenumbers and enhancements are to be noted at around 0, 500, 1500, and 1700 cm^{-1}. The red shift is due to the anharmonicity of the normal mode, while the enhancements may result from transient effects.

Though the averaged spectrum is close to ergodic, spectra calculated from individual trajectories are far from ergodic. Also, not all of the enhancements in the averaged spectrum can be seen in each trajectory. The spectrum calculated from one trajectory is shown in Figure 3b. The 14th, 4th, 26th, and 50th trajectories were selected, which are the typical spectra peaking at 0, 500, 1500, and 1700 cm^{-1}, respectively. Note that the vertical scale is different from that used in Figure 3a.

To assign peaks in the reference spectra to the normal vibrational modes of the cis isomer, harmonic reference analysis was introduced. The detailed procedure of the analysis is

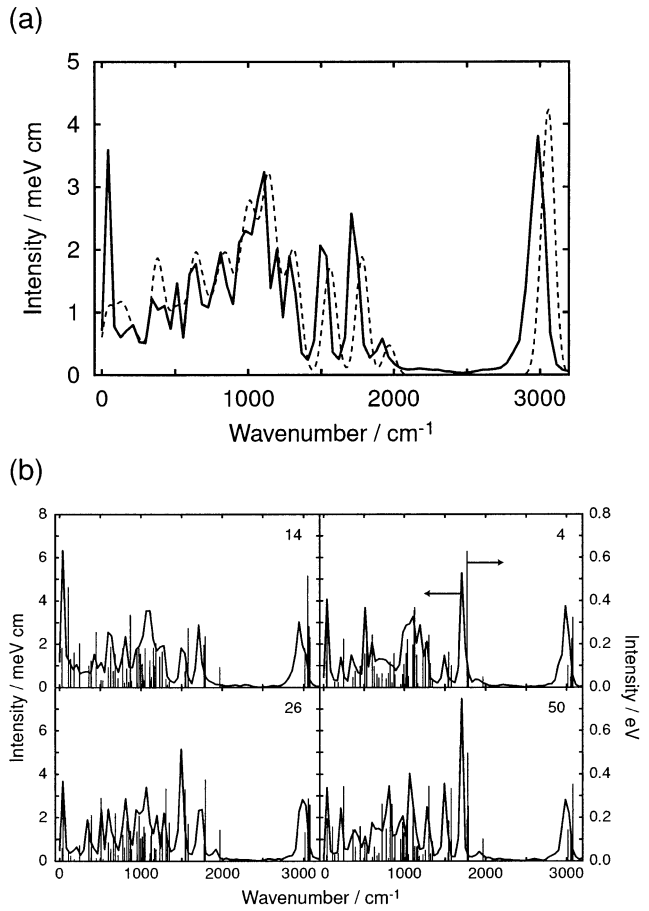

Figure 3. Transient vibrational spectra derived from the velocity autocorrelation function. The vibrational kinetic energy spectra are calculated from a time interval from 0.61 to 1.39 ps of the trajectories after the passage of the transition state to the cis side. Panel a shows the averaged transient spectrum. The ergodic spectrum, in which the available energy is distributed equally among all of the vibrational modes, is plotted in the broken line. Panel b shows the spectra calculated from individual trajectories. The index of the trajectory is printed at the right top. The result of the harmonic reference analysis is shown in the stick spectra, in which the total vibrational energy is assigned to each normal mode of *cis*-azobenzene.

summarized in Appendix A. Briefly, it is a method to locate the molecular structure and velocity in the phase space with respect to a reference structure. The reference structure is usually taken at one of the stationary points. The displacement from the reference structure and the atomic velocities of the MD snapshot are decomposed into normal modes defined at the reference structure. The vibrational energy is thus assigned to each normal mode on the basis of the harmonic approximation.

TABLE 2: The Assignment of the Spectral Peak in Figure 3 to Normal Modes of *cis*-Azobenzene[a]

	PM3		DFT		
wavenumber (cm^{-1})	mode	frequency (cm^{-1})	mode	frequency (cm^{-1})	description
500	12	508	12	493	Bz ν_6 ($+\nu_{16}$)
	13	532	13	531	Bz ν_6 ($+\nu_{16}$) + C−N=N bending
1500	48	1537	48	1450	Bz ν_{19}
	49	1546	49	1457	Bz ν_{19}
	50	1578	50	1476	Bz ν_{19} + C−N stretch
	51	1579	51	1482	Bz ν_{19} + C−N stretch
1700	52	1772	53	1587	Bz ν_8
	53	1778	54	1593	Bz ν_8
	54	1787	55	1607	Bz ν_8 + C−N stretch
	55	1788	56	1611	Bz ν_8 + C−N stretch

[a] The location of the peak (wavenumber), the assigned normal mode, and its frequency are listed. The corresponding normal mode and frequency calculated at the DFT (PW91/6-31G(d)) level are also listed. The characters of the modes are described with respect to the normal mode of benzene in the last column.

The result of the analysis is also shown in Figure 3b. Bearing the spectral shift in mind, it is possible to assign peaks in the velocity autocorrelation spectrum to the normal modes. In this way, the 0 cm^{-1} peak in the 14th trajectory is assigned to mode 3, the 500 cm^{-1} peak in the 4th to mode 13, the 1500 cm^{-1} peak in the 26th to mode 48, and the 1700 cm^{-1} in the 50th to mode 53.

After examining several other trajectories, the peaks at 500, 1500, and 1700 cm^{-1} were assigned as shown in Table 2. These modes are mostly composed of the skeletal vibrations of the benzene ring. Taking the normal modes of the benzene molecule as a reference,[19] the 500 cm^{-1} peak corresponds to in-plane bending mode (ν_6) and the 1500 and 1700 cm^{-1} peaks correspond to in-plane stretching modes (ν_{19} and ν_8, respectively). These relevant modes in benzene are depicted in Figure 4, along with the calculated and experimental frequencies. Note that PM3 method overestimates the frequency of ν_8 by nearly 200 cm^{-1}, as it also does the modes assigned to the 1700 cm^{-1} peak.

The transient spectra were also calculated at $t = 2, 3, ..., 10$ ps and averaged. Those spectra are almost identical to the one at $t = 1$ ps, except for the decrease of the 0, 1500, and 1700 cm^{-1} peaks and overall increase in the 500−1000 cm^{-1} region. The peak intensities are plotted as a function of time in Figure 5. The intensities are obtained by integrating the spectrum over an 80 cm^{-1} range for 0 and 500 cm^{-1} peaks and over a 120 cm^{-1} range for the 1500 and 1700 cm^{-1} peaks. Those intensities

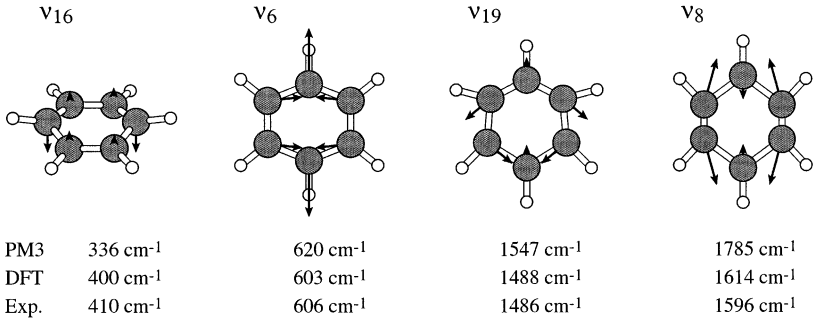

Figure 4. The normal vibrational modes of the benzene molecule, ν_{16}, ν_6, ν_{19}, and ν_8. The normal mode coordinate is indicated by arrows, and the molecular structure is deformed along the coordinate. The experimental vibrational frequency of the mode is also shown below the figure, along with those calculated by PM3 and DFT.

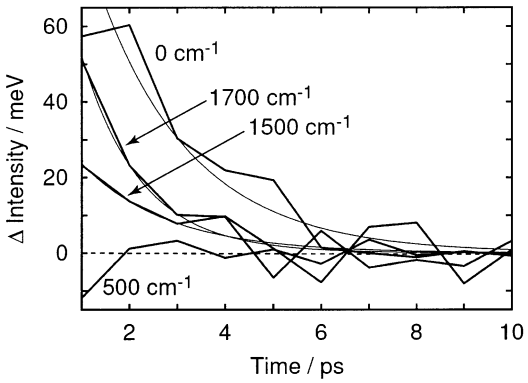

Figure 5. Integrated peak intensities plotted as a function of time for 0, 1700, 1500, and 500 cm^{-1} peaks from top to bottom. Baseline of the curve was shifted such that the averaged intensities for time $\geq$ 6 ps becomes zero. The fitted exponential decay curves are also plotted in thin lines for the 0, 1500, and 1700 cm^{-1} cases.

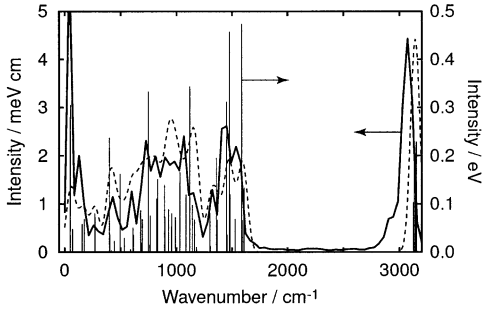

Figure 6. The transient vibrational spectrum calculated from the DFT trajectory. The ergodic spectrum, in which the available energy is distributed equally among normal modes, is plotted in a broken line. The stick spectra shown in thin lines are the result of the harmonic reference analysis, in which the vibrational energy is assigned to each normal mode of *cis*-azobenzene. The normal modes were calculated at the DFT level.

decay almost completely at around $t = 5$ ps, and fluctuation in the intensity is observed after that. The asymptotic limit of the intensity was thus determined by averaging over $t \geq 6$ ps to be 127, 103, 165, and 161 meV for the 0, 500, 1500, and 1700 cm^{-1} peaks, respectively. Taking these values as baseline, the lifetimes of the decay curves were estimated to be 2.0, 1.8, and 1.2 ps for 0, 1500, and 1700 cm^{-1} peaks. The lifetimes are considerably shorter than those reported by Tanaka et al.,[20] which may be due to the large amount of the vibrational energy employed in the present study.

The assignment of the soft modes is somewhat awkward with the present analysis, but the 0 cm^{-1} peak may be assigned to modes 1 and 3, which are the rotations of the benzene rings about the C−N axis. As can be seen in Figure 3b, there is a peak at 0 cm^{-1} for almost all of the trajectories, though they are not so prominent as that in the 14th trajectory. Most of them were assigned to mode 2, the flapping motion of the benzene rings. These assignments of the soft modes accord well with the visual intuition from the MD trajectories.

IV. Discussions

A. Transition-State Structure. At the transition state, one of the C−N bonds is aligned with the N═N bond, forming a linear structure (see Figure 1). The structure, as well as the direction, of the reaction coordinate supports the idea that isomerization proceeds not by the rotation mechanism but by inversion, in agreement with previous work.[3−8] The inversion mechanism is also confirmed in actual MD calculations; we have selected a candidate for the transition state from the trajectory that was set up for the isomerization reaction to take place and optimized it to obtain the same structure. Observations of the high-temperature trajectories (see section IV.C) also support the mechanism. As shown in Table 1, the C−N bond aligned with N═N bond is shortened, indicating that the lone pair electrons on N contribute to the C−N bonding. Because the C−N bond has nearly double bond character, C−C bonds directly connected to it are elongated considerably, as shown in Figure 1c,f. The same deformation of the benzene ring is observed at the cis stable structure if normal modes 50, 51, 54, or 55 or a combination of them are excited, which are related to ν_{19} and ν_8 modes of the benzene molecule. It is our conjecture that the deformation of the benzene ring at the transition-state structure brings about localization of the vibrational energy into these modes. And in reverse, excitation of these modes may assist the molecule to reach the transition state.

B. Force Field. Though the PM3 force field reproduces the global landscape of the potential energy surface for azobenzene adequately, there are, of course, limitations. As shown in Table 2, errors in the vibrational frequencies are about 100−200 cm^{-1}. The worst case is the frequency of N═N bond, which PM3 (1968 cm^{-1}) overestimates by more than 400 cm^{-1} compared with the DFT result (1528 cm^{-1}). These errors disturb the ordering of the vibrational modes and may mangle coupling among the modes.

To assess the reliability of the PM3 force field, two trajectories were calculated under the DFT force field. Armstrong et al.[21] state that a diffuse basis function is necessary on the nitrogen atom to describe the N═N bond in their MP2 study. On the other hand, Biswas and Umapathy[22] have shown that the density functional theory with 6-31G(d) basis set reproduces the vibrational frequencies fairly well. In the present study, we used PW91 functionals with 6-31G(d) basis sets. The trajectories were started from the DFT transition structure and ran for 1.58 ps. The deviations in the total energy were less than 125 meV. The transient spectrum at around 1 ps was calculated from one of the trajectories and is shown in Figure 6. The ergodic spectrum is also plotted by distributing the available energy of 6.07 eV equally among normal modes calculated at the DFT level.

By comparing two spectra, we notice the enhancement of the transient spectrum at the 1500 cm^{-1} peak. It was assigned to normal modes 48, 50, and 53 through the harmonic reference analysis, which is also depicted in the figure. In agreement with the PM3 result, the assigned modes are mostly composed of ν_{19} and ν_8 of the benzene ring (see Table 2). The similar features could be observed for the other trajectory (not shown in the figure). As shown in Figure 4, the frequencies of ν_{19} and ν_8 are shifted by about 100 and 200 cm^{-1}, respectively, if the level of theory is improved from PM3 to DFT. It is also true in the azobenzene molecule, so the ν_{19} related peak (1500 cm^{-1}) and ν_8 related peak (1700 cm^{-1}) in PM3 are merged at around 1500 cm^{-1} in the DFT calculation.

The observation above was derived from only a few trajectory calculations and is thus far from definitive. Looking at Figure 1f, however, we see the deformation of the benzene ring to be more prominent in the DFT calculation. Because the deformation is closely related to ν_{19} and ν_8 modes of the benzene molecule, the localization of the vibrational energy into those modes will become more probable.

C. Full Reaction. The analysis thus far has been limited to the half-reaction starting from the transition state. In the real system, however, isomerization does not necessarily proceed

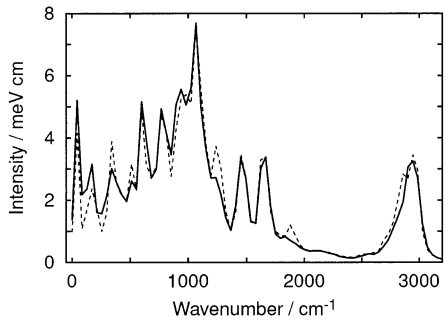

Figure 7. Transient spectrum at 1 ps before the isomerization reaction. Full-reaction trajectories were used to calculate the spectrum. The vibrational spectrum calculated at arbitrary points on nonreactive trajectories is also plotted in a broken line.

through the transition state. To check the consistencies between the half-reaction and the full reaction, trajectory calculations at high temperature, at which isomerization readily takes place, were performed.

The trajectories were started from the cis stable structure. Vibrational quanta corresponding to 1500 K were excited for each normal mode. The total vibrational energy including zero-point energy was 13.4 eV. The vibrational energy was assigned as initial kinetic energy, and the direction of the velocity vector was chosen randomly for each mode. A warmup period of 7.6 ps was employed; the trajectories reacted within the period were discarded. This period is long enough at least for the high-frequency mode because the lifetime of the vibrational decay will be 1−2 ps as shown in section III.C. The trajectories were then pursued for another 7.6 ps, and those reacted within the period were picked up.

A total of 50 trajectories were calculated: 14 reacted, 14 not reacted, and the rest of the trajectories were terminated during the warmup period. For the reactive trajectories, the transient vibrational spectrum was calculated at 1 ps before the reaction. For the nonreactive trajectories, the vibrational spectrum was calculated arbitrarily at 7.6 ps to obtain the ordinary vibrational spectrum as a reference. The spectra were averaged and are plotted in Figure 7. Unfortunately, the transient spectrum is almost identical to the ordinary spectrum, except for the enhancement near 0 cm^{-1}. This result suggests that the story for the (high-energy) full reaction might be different from the (low-energy) half-reaction. It must be noted, however, that the vertical scale is different from Figure 3a and over all vibrational excitation in Figure 7 is considerably above the former. Thus subtle differences will be buried. Furthermore, the fluctuation of the peak intensities among the individual spectra are as large as those in Figure 3b, indicating a similar coupling scheme among the vibrational modes.

V. Conclusion

The thermal isomerization of *cis*-azobenzene was studied by the direct molecular dynamics method with a force field calculated by a semiempirical molecular orbital method. An unconventional numerical integrator[14] was employed that enabled us to use a larger integration step. The transition-state structure of the reaction was first located, and the trajectories were started from there to the cis side. The transient spectra were calculated after 1 ps, which shows that the skeletal vibrational modes of the benzene ring, namely, ν_{19} and ν_8, are excited. A similar extra feature of the spectrum was observed when a force field of higher precision, calculated by density functional theory, was used. Deformations of the benzene ring at the transition state were found to relate closely to ν_{19} and ν_8, which may explain the enhancement of those modes. Some trajectories were also calculated with high internal energy to accelerate isomerization, but such enhancement could not be seen in those trajectories.

The present study indicates that ν_{19} and ν_8 modes of the benzene ring play an important role in the thermal isomerization reaction of the azobenzene molecule. The similar modes are known to accelerate the isomerization reaction of azodendrimer.[2] In the latter case, however, the vibrational modes seem to survive for several microseconds, while the lifetime of the modes in azobenzene are on the order of picoseconds. The effect of the steric restriction posed by the dendrimer shell on the vibrational lifetime is now under investigation.

Acknowledgment. N.K. thanks the Ministry of Education, Science, Sports and Culture of Japan for a visiting research fellowship at the University of Puerto Rico.

Appendix A: Harmonic Reference Analysis

Given the structure and atomic velocity, the harmonic reference analysis locates the structure of the target molecule in phase space with respect to a reference point. The stationary structure is used as reference point, of which the normal modes are known a priori. The displacement of atoms from the reference structure is decomposed into the normal modes, as well as the velocity. The vibrational energy and phase is thus assigned for each normal mode under the harmonic approximation.

The actual procedure is divided into two steps: taking alignment of the target structure to the reference and decomposition of the displacement/velocity into the normal modes. The following conventions are used in this section: N = number of atoms; i = index of atoms, $1 \le i \le N$; $\mathbf{x}_i^0$ = atomic Cartesian coordinate of the reference structure; $\mathbf{x}_i$ = atomic Cartesian coordinate of the target structure; $\mathbf{v}_i$ = atomic Cartesian velocity of the target structure; $\mathbf{n}_k$ = unit rotational vector, $k = x, y$, and z; p = index of normal modes, $1 \le p \le 3N - 6$; $\mathbf{u}_p^0$: $3N$-dimensional normal-mode vector; $[\mathbf{x}_i] = 3N$-dimensional vector collected over $\mathbf{x}_i$.

1. Alignment. There are $3N - 6$ normal modes in an N-atom molecule, where three translational and three rotational degrees of freedom are removed. To decompose the structural displacement into the normal modes, the target molecule should be aligned to the reference structure such that translational/rotational components are excluded from the displacement vector. The exclusion of the translational modes is simple: place the center-of-mass of both the target and reference structures at the same point. The rest of the discussion is devoted to the exclusion of the rotational modes.

First, the spatial coordinate and velocity are transformed into mass-weighted coordinates,

$$\tilde{\mathbf{x}}_i = \sqrt{m_i}\mathbf{x}_i \tag{A1}$$

In the mass-weighted coordinate system, the normal-mode vectors form an orthonormal set. They are also orthogonal to the rotational modes,

$$\tilde{\mathbf{u}}_p^0 \cdot [\mathbf{n}_k \times \tilde{\mathbf{x}}_i^0] = 0 \tag{A2}$$

Therefore, by definition, the orientation of the target structure

is aligned to the reference if

$$0 = [\tilde{\mathbf{x}}_i - \tilde{\mathbf{x}}_i^0]\cdot[\mathbf{n}_k \times \tilde{\mathbf{x}}_i^0]$$
$$= [\tilde{\mathbf{x}}_i]\cdot[\mathbf{n}_k \times \tilde{\mathbf{x}}_i^0] \quad \text{(A3)}$$

The rotation angle θ_k around $\mathbf{n}_k$ is chosen such that eq A3 is satisfied. If θ_k is small, the atomic coordinate of the target changes as

$$\tilde{\mathbf{x}}_i \rightarrow \tilde{\mathbf{x}}_i + (\mathbf{n}_k \times \tilde{\mathbf{x}}_i)\theta_k \quad \text{(A4)}$$

Putting eq A4 to A3, we get

$$\theta_k = \frac{[\tilde{\mathbf{x}}_i]\cdot[\mathbf{n}_k \times \tilde{\mathbf{x}}_i^0]}{[\tilde{\mathbf{x}}_i]\cdot[\tilde{\mathbf{x}}_i^0 - (\tilde{\mathbf{x}}_i^0\cdot\mathbf{n}_k)\mathbf{n}_k]} \quad \text{(A5)}$$

Equations A4 and A5 should be iterated until θ_k becomes small enough. Starting from the moderate orientation, the alignment condition is met within a few iterations in most cases.

The exclusion of translational/rotational motion from the velocity vector is trivial. It is even not necessary if the target structure is selected from MD trajectories of which the total momentum and total angular momentum are taken to be zero.

2. Decomposition. The decomposition of the displacement and velocity vector into the normal modes is reduced to the simple projection in the mass-weighted coordinate system,

$$q_p = \tilde{\mathbf{u}}_p\cdot[\tilde{\mathbf{x}}_i - \tilde{\mathbf{x}}_i^0] \quad \text{(A6)}$$

$$\dot{q}_p = \tilde{\mathbf{u}}_p\cdot[\tilde{\mathbf{v}}_i] \quad \text{(A7)}$$

where q_p and $\dot{q}_p$ are the (mass-weighted) normal coordinate. The vibrational Hamiltonian under the harmonic approximation is written as

$$H = \sum_p h_p \quad \text{(A8)}$$

$$h_p = \frac{1}{2}\dot{q}_p{}^2 + \frac{1}{2}\omega_p{}^2 q_p{}^2 \quad \text{(A9)}$$

where ω_p is the angular frequency of the pth normal mode and h_p is the vibrational energy assigned to the mode. The phase for the mode is determined as

$$\phi_p = \tan^{-1}\frac{\dot{q}_p}{\omega_p q_p} \quad \text{(A10)}$$

3. Remedy for Anharmonicity. Different from the velocity autocorrelation function method, harmonic reference analysis can derive the vibrational energy for each normal mode just from a snapshot of MD trajectories. It is made possible by utilizing the information on the harmonic potential energy surface near the reference structure. There is a caveat, however, especially when the molecule has soft modes. The large amplitude motion of the soft mode takes the molecule far away from the reference structure. There, the couplings among the modes deteriorate the set of normal mode, which is defined with respect to the reference structure. Furthermore, the potential energy term in eq A9 becomes unreliable where q_p is far from zero because of the anharmonicity of the mode. To reduce these defects, the application of the analysis was limited to situations in which the MD trajectory comes close to the reference structure. In addition, the MD structures were scanned near there, and the kinetic part of eq A9 was maximized for each mode.

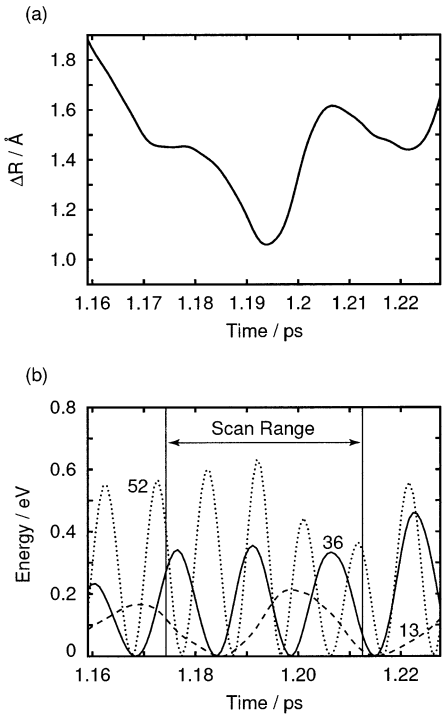

Figure 8. Harmonic reference analysis for a MD trajectory. The cis stable structure is taken as the reference. In panel a, the displacement from the reference structure, ΔR, is plotted as a function of time. The orientation of the MD structure is aligned to the reference. In panel b, the kinetic energies assigned to normal modes are plotted as a function of time. The kinetic energies of modes 13, 36, and 52 are plotted in broken, solid, and dotted lines, respectively. The scan range, for which the maximum value of the kinetic energy is sought, is also indicated in the figure.

The actual process of the analysis is depicted in Figure 8 taking the fourth trajectory shown in Figure 3b as an example. The cis stable structure was used as the reference. In Figure 8a, the $3N$-dimensional distance between the MD structure and the reference one,

$$\Delta R = |[\mathbf{x}_i - \mathbf{x}_i^0]| \quad \text{(A11)}$$

is plotted as a function of time. The distance reaches its minimum at 1.19 ps. The kinetic energies assigned to the normal mode 13 (532 cm^{-1}), 36 (1122 cm^{-1}), and 52 (1772 cm^{-1}) are plotted in Figure 8b. Centered at the ΔR minimum, the range of ± 0.02 ps (± 25 steps) was selected to seek the maximum of the kinetic energies. In this way, the vibrational energies of 0.21, 0.36, and 0.63 eV were assigned to mode 13, 36, and 52, respectively.

Appendix B: Unit System Used in the Work

In the actual calculation, the following unit system was used throughout: for length, 1 Å $= 10^{-10}$ m; for mass, 1 amu $\simeq 1.660\,54 \times 10^{-27}$ kg; for time, 1 $\tau \simeq 1.018\,05 \times 10^{-14}$ s; for charge, 1 e $\simeq 1.602\,18 \times 10^{-19}$ C. With this unit system, the unit of energy becomes 1 eV $= 1.602\,18 \times 10^{-19}$ J. The unit system is designed for the convenience to describe molecular systems. Some of the physical constants in the unit system are listed as follows: Planck constant, $\hbar \simeq 6.465\,41 \times 10^{-5}$; Boltzmann constant, $k_B \simeq 8.617\,34 \times 10^{-5}$; speed of light, $c \simeq 3.052\,04 \times 10^{4}$; electric constant, $\epsilon_0 \simeq 5.526\,35 \times 10^{-3}$. The

dimensions of these values are the same as those in the MKSA unit system. The integration step used in the present work was actually taken to be 0.075τ. That is why it is not 0.75 fs exactly.

References and Notes

(1) Liu, Z. F.; Hashimoto, K.; Fujishima, A. *Nature* **1990**, *347*, 658. Sekkat, Z.; Dumont, M. *Appl. Phys. B* **1992**, *54*, 486. Ikeda, T.; Tsutsumi, O. *Science* **1995**, *268*, 1873. Willner, I.; Rubin, S.; Riklin, A. *J. Am. Chem. Soc.* **1991**, *113*, 3321. Tirelli, N.; Altomare, A.; Ciardelli, F.; Solaro, R. *Can. J. Chem.* **1995**, *73*, 1849.

(2) Jiang, D.-L.; Aida, T. *Nature* **1997**, *388*, 454.

(3) Andersson, J.-Å.; Petterson, R.; Tegnér, L. *J. Photochem.* **1982**, *20*, 17.

(4) Rau, H.; Lüddecke, E. *J. Am. Chem. Soc.* **1982**, *104*, 1616.

(5) Ljunggren, S.; Wettermark, G. *Acta Chem. Scand.* **1971**, *25*, 6.

(6) Cimiraglia, R.; Hofmann, H.-J. *Chem. Phys. Lett.* **1994**, *217*, 430.

(7) Cattaneo, P.; Persico, M. *Phys. Chem. Chem. Phys.* **1999**, *1*, 4739.

(8) Ishikawa, T.; Noro, T.; Shoda, T. *J. Chem. Phys.* **2001**, *115*, 7503.

(9) Biswas, N.; Umapathy, S. *J. Chem. Phys.* **1997**, *107*, 7849.

(10) Fujino, T.; Tahara, T. *J. Phys. Chem. A* **2000**, *104*, 4203.

(11) Tachikawa, H. *J. Phys. Chem. A* **1998**, *102*, 7065. Tachikawa, H. *Phys. Chem. Chem. Phys.* **2000**, *2*, 4702. Aida, M.; Yamataka, H.; Dupuis, M. *Chem. Phys. Lett.* **1998**, *292*, 474. Ishikawa, Y.; Binning, R. C., Jr.; Shramek, N. S. *Chem. Phys. Lett.* **1999**, *313*, 341. Ishikawa, Y.; Gong, Y.; Weiner, B. R. *Phys. Chem. Chem. Phys.* **2000**, *2*, 869. Ishikawa, Y.; Binning, R. C., Jr.; Ikegami, T. *Chem. Phys. Lett.* **2001**, *343*, 413.

(12) Stewart, J. J. P. *J. Comput. Chem.* **1989**, *10*, 209. Stewart, J. J. P. *J. Comput. Chem.* **1989**, *10*, 221.

(13) Perdew, J. P.; Chevary, J. A.; Vosko, S. H.; Jackson, K. A.; Pederson, M. R.; Singh, D. J.; Fiolhais, C. *Phys. Rev. B* **1992**, *46*, 6671.

(14) Martyna, G. J.; Tuckerman, M. E. *J. Chem. Phys.* **1995**, *102*, 8071. There is a typo in eq 2.16: "2" in the denominator of the last equation is not necessary.

(15) Frisch, M. J.; Trucks, G. W.; Schlegel, H. B.; Scuseria, G. E.; Robb, M. A.; Cheeseman, J. R.; Zakrzewski, V. G.; Montgomery, J. A., Jr.; Stratmann, R. E.; Burant, J. C.; Dapprich, S.; Millam, J. M.; Daniels, A. D.; Kudin, K. N.; Strain, M. C.; Farkas, O.; Tomasi, J.; Barone, V.; Cossi, M.; Cammi, R.; Mennucci, B.; Pomelli, C.; Adamo, C.; Clifford, S.; Ochterski, J.; Petersson, G. A.; Ayala, P. Y.; Cui, Q.; Morokuma, K.; Malick, D. K.; Rabuck, A. D.; Raghavachari, K.; Foresman, J. B.; Cioslowski, J.; Ortiz, J. V.; Stefanov, B. B.; Liu, G.; Liashenko, A.; Piskorz, P.; Komaromi, I.; Gomperts, R.; Martin, R. L.; Fox, D. J.; Keith, T.; Al-Laham, M. A.; Peng, C. Y.; Nanayakkara, A.; Gonzalez, C.; Challacombe, M.; Gill, P. M. W.; Johnson, B. G.; Chen, W.; Wong, M. W.; Andres, J. L.; Head-Gordon, M.; Replogle, E. S.; Pople, J. A. *Gaussian 98*, revision A.9; Gaussian, Inc.: Pittsburgh, PA, 1998.

(16) Stewart, J. J. P. *MOPAC 2000*; Fujitsu Limited: Tokyo, Japan, 1999.

(17) Kurita, N.; Tanaka, S.; Itoh, S. *J. Phys. Chem. A* **2000**, *104*, 8114.

(18) Kurita, N.; Ikegami, T.; Ishikawa, Y. *Chem. Phys. Lett.*, in press.

(19) Wilson, E. B., Jr. *Phys. Rev.* **1934**, *45*, 706.

(20) Tanaka, S.; Itoh, S.; Kurita, N. *Chem. Phys.* **2001**, *272*, 171.

(21) Armstrong, D. R.; Clarkson, J.; Smith, W. E. *J. Phys. Chem.* **1995**, *99*, 17825.

(22) Biswas, N.; Umapathy, S. *J. Phys. Chem. A* **1997**, *101*, 5555.